Dalton Transactions

An in situ spectroelectrochemical study on the orientation changes of an $[Fe^{III}L^{N2O3}]$ metallosurfactant deposited as LB Films on gold electrode surfaces

Journal:	*Dalton Transactions*
Manuscript ID	DT-ART-01-2018-000333.R1
Article Type:	Paper
Date Submitted by the Author:	05-Mar-2018
Complete List of Authors:	Brand, Izabella; University of Oldenburg, Department of Chemistry Juhaniewicz-Debinska, Joanna; University of Warsaw, Faculty of Chemistry, Biological and Chemical Research Centre Wickamasinghe, Lanka; Wayne State University, Chemistry Verani, Claudio; Wayne State University, Chemistry

Journal Name

ARTICLE

An *in situ* spectroelectrochemical study on the orientation changes of an $[Fe^{III}L^{N2O3}]$ metallosurfactant deposited as LB Films on gold electrode surfaces

Received 00th January 20xx,
Accepted 00th January 20xx

DOI: 10.1039/x0xx00000x

www.rsc.org/

Izabella Brand,[a,*] Joanna Juhaniewicz-Debinska,[b] Lanka Wickramasinghe,[c] and Claudio N. Verani,*[,c]

In this paper we analyze the changes in molecular orientation triggered by electrochemical reduction of an iron-containing surfactant in Langmuir-Blodgett films deposited onto gold electrodes. The metallosurfactant $[Fe^{III}(L^{N2O3})]$ (**1**) is an established molecular rectifier capable of unidirectional electron transfer between two electrodes. A gradual decrease in the activity is observed in sequential current *vs.* potential curves upon repeated cycles. Here we evaluate the redox response associated with the reduction of the Fe^{III}/Fe^{II} couple in a single monolayer, as well as in a 5-layer LB film of **1**. We use polarization modulation infrared reflection absorption spectroscopy (PM IRRAS) to follow structural and orientation changes associated with such applied potential scans. We observe that the reduction of the Fe center becomes increasingly irreversible because an Fe-$O_{phenolate}$ bond is cleaved. This transformation is accompanied by an almost vertical change in the orientation of metallosurfactant molecules in LB films.

Introduction

Five-coordinate iron(III) surfactants show some unusual redox and spectroscopic behavior.[1-4] In these species a high-spin Fe^{III} ion binds to phenolate-rich amphiphilic ligands of low-symmetry and forms species such as $[Fe^{III}(L^{N2O3})]$, **1**, [1, 3](shown in **Figure 1a**) and $[Fe^{III}(L^{N2O2})Cl]$, **2**.[1, 2, 4] These species act as diode-like metallosurfactants capable of current rectification, or unidirectional transfer of electrons, when deposited as Langmuir-Blodgett (LB) monolayers between two gold electrodes in an Au|LB|Au device. This molecular current rectification was confirmed when the $[Fe^{III}(L^{N2O2})Cl]$ (**2**) species was assembled using a eutectic GaIn|LB|Au device.[4] Further studies propose that directional electron transfer takes place through singly-occupied molecular orbitals (SOMO) with predominant metallic character, rather than *via* the expected unoccupied MOs. As a consequence, an appropriate matching gap is required between the Fermi levels of the electrode and the SOMOs of the complex in order to enable rectification.

Experimental and theoretical evidence for both metallosurfactants **1** and **2** position the SOMO of the molecular diode at 1.0 to 1.2 eV above the unbiased Fermi level of the gold electrode.

The SOMO is better described as a linear combination of the $3d_{xz}$ and $3d_{yz}$ MOs, the lowest lying metal-based orbitals in a five-coordinate Fe^{III} ion with an approximate square pyramidal C_{4v} symmetry with idealized $e(d_{xz}^1 + d_{yz}^1)$ $b_2(d_{xy}^1)$ $a_1(d_{z2}^1)$ $b_1(d_{x2+y2}^1)$ configuration.[2, 3] Thus, rectification takes place when the lowest lying SOMO is populated (reduced) by 1 electron, followed by rapid transfer to the second Au electrode. This scenario, described as an asymmetric mechanism,[2] precludes involvement of the highest occupied ligand-based HOMO due to the large HOMO/Fermi gap. On the other hand, if this gap is narrow oxidation of the HOMO may lead to *bona fide* unimolecular mechanisms of electron transfer.[3] Therefore, rectification *via* an asymmetric mechanism can be simplified by the redox process.

$$[Fe^{III}(L^{N2O3})]^0 + e^- \rightleftharpoons [Fe^{II}(L^{N2O3})]^- \quad (1)$$

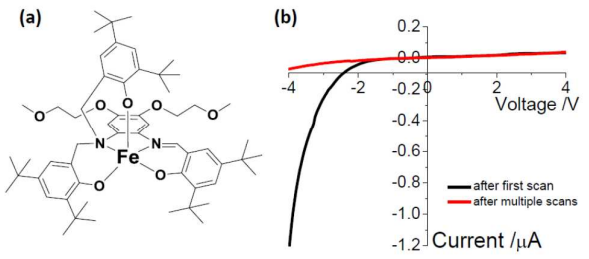

Figure 1. (a) The structure of the metallosurfactant $[Fe^{III}(L^{N2O3})]$, **1**; (b) Comparison of current/voltage plots of a monolayer of **1** after one (black trace) and after five (red trace) scans.

[a] *Department of Chemistry, Carl von Ossietzky University, 26111 Oldenburg, Germany.*
[b] *Faculty of Chemistry, Biological and Chemical Research Centre, University of Warsaw, Zwirki i Wigury 101, 02089 Warsaw, Poland.*
[c] *Department of Chemistry, Wayne State University, 5101 Cass Ave, Detroit, MI 48202.*

Electronic Supplementary Information (ESI): Monolayer characterizations, capacitance-potential curves, isotropic optical constants, deconvolution procedure, and additional PM-IRRA spectra of LB films of $[Fe^{III}(L^{N2O3})]$

Ultimately, the measurement of multiple rectification cycles leads to considerable loss of activity in the device, as shown in **Figure 1b**. This redox process leads to a charge imbalance between the dicationic Fe^{II} ion and the trianionic ligand $(L^{N2O3})^{3-}$ prompting changes to the chemical liability of the metal-ligand bonds and coordination preferences. Such processes may lead to slow degradation of the molecular diode by geometrical changes that compromise electron transfer.

In this paper we present an *in situ* spectroelectrochemical evaluation of the orientation and structural changes triggered by unidirectional electron transfer in LB Films of **1** on gold electrodes. We proceed by using polarization modulation infrared reflection absorption spectroscopy (PM IRRAS), an excellent analytical tool for studies of potential-driven changes in the composition and structure of redox-active films on surfaces.[5] This study is a pioneering approach to shed light in the behavior of diode-like LB films during the process of current rectification.

Results and discussion

Monolayer properties of $[Fe^{III}(L^{N2O3})]$. The species $[Fe^{III}(L^{N2O3})]$, **1**, was obtained as reported elsewhere.[1, 6, 7] In brief, the neutral and triply protonated ligand H_3L^{N2O3} was obtained by treatment of 4,5-dinitrobenzene-1,2-diamine with 2,4-di-*tert*-butyl-6-(chloro methyl) phenol in methanol under reflux. Complex **1** was obtained by treating one equiv. of the purified ligand with one equiv. of an iron(III) salt in presence of anhydrous $NaOCH_3$. This species forms stable monolayers at the air|water interface.[1] A description of the monolayer behavior of $[Fe^{III}(L^{N2O3})]$ at room temperature is summarized as follows: the lift-off area, corresponding to the area per molecule at which the surface pressure starts to increase and where intermolecular interactions are detected, is equal to 2.3 nm^2 (see Supporting Information, **Figure S1**); at a surface pressure of 20 – 25 mN m^{-1} and corresponding area per molecule ranging from 1.4 to 1.0 nm^2, a discontinuity is observed indicative of a phase transition in the monolayer. Afterwards the surface pressure increases to *ca.* 55 – 60 mN m^{-1}. The Langmuir monolayer collapses when an average area per molecule of 0.64 ± 0.04 nm^2 is reached. The compressibility modulus K_s for the monolayer of **1** varies between 45 – 60 mN m^{-1} and is given by $K_s = [-(1/A)(dA/d\pi)]^{-1}$ were A is the molecular area and π is the corresponding surface pressure (**Figure S1**). A phase transition at areas greater than 1.0 nm^2 does not lead to apparent changes of K_s, indicating that the molecules of **1** in the monolayer exist in a two dimensional liquid-like state. The monolayer was compressed to π = 33 mN m^{-1} and transferred onto the Au electrode surface in order to investigate the impact of redox changes in the structure and orientation of the molecules of **1** in LB monolayer and multilayer assemblies.

Electrochemistry of LB films of $[Fe^{III}(L^{N2O3})]$. Cyclic voltammetry experiments were used to characterize both the monolayer and 5-layer LB films of **1** on the Au electrode surface (**Figure 2**). An increase in the Faradaic current is observed only in the first negative-going potential sweep.[6] In the monolayer of **1**, two reduction peaks are seen at E_{c1} = -0.255 and E_{c2} = -0.680 V in the first negative-going potential scan (**Figure 2a**). In the following positive-going potential scan, an anodic peak of small amplitude is observed at E_{a2} = -0.470 V. However, in the subsequent scan no redox activity of **1** is observed. Similar to the monolayer, the CV of **1** in the 5-LB film, shows in the first negative-going potential scan one reduction peak at E_c = –0.410 V (**Figure 2b**). However, no Faradaic current associated with the oxidation reaction is observed in the following positive-going potential scan. Phenolate-rich coordination compounds are known for their complex electrochemical behavior.[6, 8-11] The uptake of one electron from the electrode leads to the reduction of the metal ion. Alternatively reduction of the ligand may occur[6, 12] at considerably more negative potentials.[13] Thus the reduction of **1** in the LB films is ascribed to the Fe^{III}/Fe^{II} couple. Integration of the Faradaic current over time provides the charge associated with reduction and allows for the calculation of the surface concentration of electroactive **1** in the LB film adsorbed on the Au surface (**Table 1**).

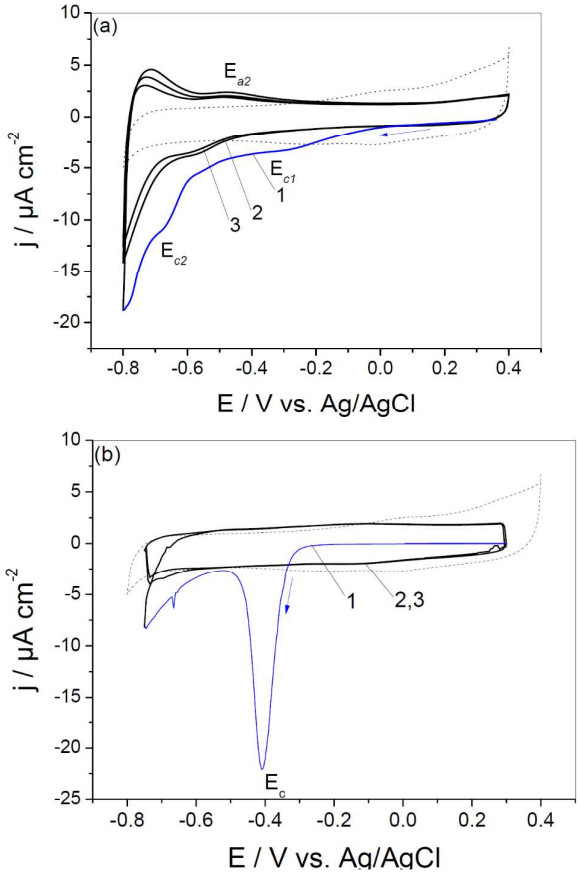

Figure 2. Cyclic voltammograms of (a) LB monolayer and (b) LB 5-layers of **1** deposited on the Au electrode surface in 0.05 M NaF electrolyte solution; 50 mV s^{-1} scan rate; full lines 1, 2, 3:

Table 1. Data obtained from electrochemical experiments on LB films of **1** on Au.

	Q_{red} ($\mu C\ cm^{-2}$)	Γ ($mol\ cm^{-2}$)[1]	Mma (nm^2)	$\Gamma_{expected}$ * ($mol\ cm^{-2}$)	% electro-activity
1LB	10.90 ± 1.00	1.1×10^{-10}	1.46	1.7×10^{-10}	67.0
5LB	18.60 ± 0.60	1.9×10^{-10}	0.86	8.5×10^{-10}	22.8

* Surface coverage expected from the LB transfer conditions at π = 33 mN m^{-1} and corresponding area per molecule A = 0.98 nm^2.

This disparity indicates that not all molecules present in the film undergo reduction. In the case of the LB monolayer, *ca.* 67% of molecules are reduced in two reduction steps. This could be attributed to the presence of inhomogeneities of distribution associated with orientation variability of the electroactive Fe^{III} ion centers with respect to the Au electrode surface. In the case of the 5-layer LB film, just over 20% of **1** shows electrochemical response. This relatively low electroactivity suggests that only the molecules under direct contact with the Au surface undergo reduction. Electrochemical measurements indicate also that reduction is associated with an increase in the capacitance of the LB-modified electrode (**Figure S2**). In the first negative-going potential scan at E > -0.2 V the capacitance of the monolayer of **1** is close to 11 µF cm^{-2}. At E < -0.2 V capacitance starts to increase gradually with a negative potential shift. In the 5LB film the initial capacitance is equal to 0.35 µF cm^{-2}. Reduction leads to formation of a new state in the LB film observed as an abrupt capacitance increase to 13 µF cm^{-2}. Further negative potential shift results in capacitance values characteristic of the unmodified Au electrode in NaF electrolyte. Merging of the capacitance curves for modified and unmodified electrodes strongly suggests potential-driven desorption of **1** from the surface.[14] The capacitance decreases during the successive positive potential scan at E > -0.3 V, thus indicating resorption of **1** onto the Au surface (**Figure S2**). In the re-adsorbed films the capacitance minimum is in the range of 12 – 16 µF cm^{-2}. Considering these results we propose that the incremental loss of activity observed during rectification with LB films of **1** is not caused by irreversible detachment of the molecules from the surface of the electrode. In order to probe other potential sub-molecular scale changes, PM IRRA spectra in the C-O, ring stretching, and CH stretching mode regions were recorded upon potential scans. These results provide a comprehensive picture of potential-dependent changes in LB films of **1**.

PM-IRRAS of LB films of [$Fe^{III}(L^{N2O3}$)] under applied potential scans. **Figure 3** shows the PM IRRA spectra of the monolayer in the 1350 – 1100 cm^{-1} spectral region. A calculated PM IRRA spectrum of randomly distributed molecules of **1** in a monolayer-thick film (1.90 nm as determined in an independent experiment)[1] is shown in **Figure 3a**. This spectrum was calculated from isotropic optical constants (**Figure S3**) according to well-established procedures.[15] A broad absorption mode between 1320 and 1220 cm^{-1} is composed of a few overlapped IR absorption modes. Two high frequency modes centered at 1298 and 1262 cm^{-1} arise predominantly from the C-O stretching mode of the phenolate groups.[12, 13, 16-20] The corresponding stretching mode in **1** involves the C-O-Fe vibration. Due to the heaviness of the Fe ion the Fe-O stretching mode does not contribute to this mode, but according to previous studies of phenolates, it arises from the ν(C-O) vibration.[19] The full width at half maximum (fwhm) is equal to 41.0 ± 0.6 and 34.6 ± 0.5 cm^{-1}, respectively. The presence of two ν(C-O) IR absorption modes in a solution spectrum of **1** suggests dissimilarities between the three phenolate groups. The integral intensity of the ν(C-O) at 1262 cm^{-1} is almost two times larger than the intensity of the high frequency mode at 1298 cm^{-1}, suggesting that the length of one C-O bond at the phenolate moiety differs from those at the two other groups. This is in excellent agreement with known structures of archetypical complexes[6, 7] where two of the C-$O_{phenolate}$ bonds are ca. 2-5 Å longer than the bond of the third phenolate. The IR absorption mode centered at 1240 cm^{-1} arises from the ν(C-O) mode in the short hydrophilic alkoxy chains of **1**. Broad absorption modes between 1220 – 1190 cm^{-1} have a complex origin and arise predominantly from the ν(C-C), ν(C-N), ν(C-O) stretching modes.[21] The absorption mode observed at 1168 cm^{-1} originates from C-H bending and C-C stretching. [21, 22]

In the monolayer of **1** on the Au surface the strongest contribution to *in situ* PM IRRA spectra arises from the ν(C-O) mode at 1262 ± 2 cm^{-1} (**Figures 3b,c**). The shape and intensity

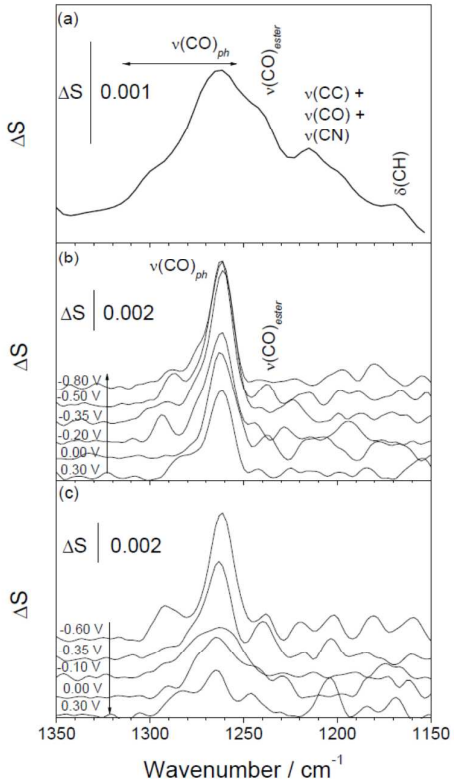

Figure 3a-c. PM IRRA spectra in 1350 – 1150 cm^{-1} spectral region of (a) randomly distributed molecules of **1** in a monolayer-thick film (d = 1.90 nm) compared to LB monolayer film of **1** on Au surface in (b) first negative scan, (c) subsequent positive scans at indicated potentials.

of this mode strongly depend on the potential applied to the Au electrode. Prior to reduction at E > -0.2 V the PM IRRA spectra show a well resolved ν(C-O) absorption mode centered at 1262 cm^{-1} and a weak shoulder at the high frequency side of the spectrum. In the first negative-going potential scan at E < -0.35 V, reduction is associated with an increase in the intensity of the ν(C-O) mode. The frequency of the ν(C-O) at 1262 cm^{-1} does not depend on the applied potential. Compared to the liquid phase spectrum, the ν(C-O) mode at 1262 cm^{-1} in the LB monolayer is narrow; its fwhm equals to 15.5 ± 1.5 cm^{-1}. A significant decrease in the fwhm of the ν(C-O) at 1263 cm^{-1} indicates that adsorbed molecules of **1** have distinct distribution and restricted mobility. Reversing the potential scan influences neither the intensity of this mode nor its fwhm, until **1** adsorbs on the Au surface. At potentials corresponding to the film resorption on the Au surface (-0.3 < E <0.0 V) the integral intensity of the ν(C-O) mode significantly decreases and its fwhm increases to 30.0 ± 3 cm^{-1} (**Figure 3c**), being comparable to the fwhm measured in the liquid phase.
Potential-driven resorption of reduced **1** indicates some changes in the rigid molecular-scale orientation in the film. In the following potential steps, the intensity of the ν(C-O) mode further decreases and cannot be distinguished from the background spectra. However, the monolayer of **1** is adsorbed on the Au electrode surface.

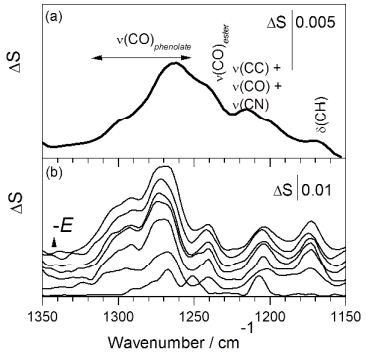

Figure 4. PM IRRA spectra in the 1350 – 1150 cm^{-1} spectral region: (a) randomly distributed molecules of **1** in a 5-monolayer thick film. 5-LB film of **1** on Au surface in (b) first negative scan at potentials 0.3, 0.0, -0.2, -0.3, 0.45, -0.5, and -0.8 V *vs.* Ag/AgCl.

Potentials applied to the 5-layers LB film on Au also cause considerable changes to the *in situ* PM IRRA spectra (**Figure 4**). Due to the larger population of molecules of **1** in 5-LB film on Au, the observed IR modes in the solution spectrum are well-resolved. The intensities of the ν(C-O) modes at 1262 and 1286 cm^{-1} increase in the first negative-going potential scan. Upon reduction at E < -0.25 V a new contribution to the ν(C-O) at 1308 cm^{-1} is observed (**Figure 4b**). A blue-shift of the ν(C-O) mode indicates a decrease of the reduced mass involved in the given vibration and/or an increase in the length of the chemical bond between the vibrating atoms. For example reduction of halogenated phenols on a palladized titanium electrode leads to a blue shift of the ν(C-O) mode from 1268 cm^{-1} in phenols to 1308 cm^{-1} in the free phenolate ion.[13] Thus, the blue shift of the high frequency ν(C-O) mode suggests that the reduction of Fe^{III} is accompanied by the cleavage of at least one Fe-O bond and formation of deprotonated phenolate groups no longer coordinated to the Fe ion in **1.** Our result suggests that uncoordinated phenolate ions are present in the hydrophobic environment of the LB multilayer. At E < -0.30 V the intensity of the ν(C-O) mode reaches a maximum and becomes independent of the potential applied to the Au electrode (**Figure 4**).

According to the IRRAS surface selection rule,[23] changes in the intensity of an IR absorption mode in organized films arise from reorientation of molecules adsorbed to the surface. In IRRAS of anisotropic films the intensity of a given IR absorption mode ($\int Adv$) depends not only on Γ, but also on the orientation of the transition dipole vector of a given vibration (μ) with respect to the electric field vector (E) (perpendicular to the surface):[23, 24]

$$\int Adv \propto \Gamma \left|\vec{\mu} \bullet \vec{E}\right|^2 = \Gamma \left|\vec{\mu}\right|^2 \left|\vec{E}\right|^2 \cos^2\theta \qquad (2)$$

The angle θ between the two vectors can be calculated from equation 3:

$$\cos^2\theta = \frac{\int A_{exp}\, dv}{\int A_{random}\, dv} \qquad (3)$$

The terms $A_{exp}dv$ and $A_{random}dv$, respectively represent the intensities of the corresponding IR absorption modes of monolayer assemblies of **1** on Au and of randomly distributed **1** in a LB-thick film.
In **1** three phenolate groups have well defined orientation [see the X-ray crystal structure in reference 1]. Two phenolate groups C-O-Fe-O-C lie in one plane whereas the third Fe-O-C group is almost at right angles to this imaginary plane. The calculated tilt angle $\theta_{\nu(C\text{-}O)}$ represent an average orientation of the three phenolte groups in **1** in LB films. Changes of the calculated $\theta_{\nu(C\text{-}O)}$ as a function of the electrode potential in the 1LB and 5LB films of **1** are shown in **Figure 5**.
The values of $\theta_{\nu(C\text{-}O)}$ angles depend on the potential applied to

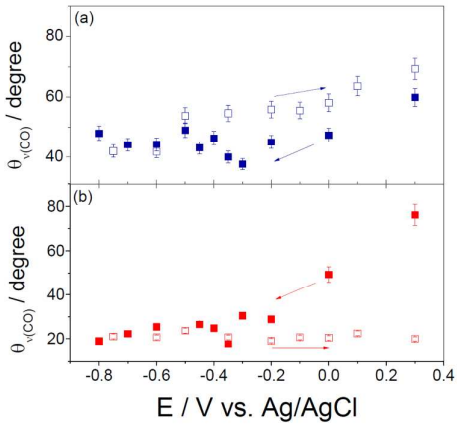

Figure 5a-b. Plots of the angle $\theta_{\nu(CO)}$ mode *vs*. E applied to the Au electrode in (a) monolayer and (b) 5-LB film of **1** adsorbed on Au; filled points: first negative-going, opened points: subsequent positive-going potential scans.

the electrode and on the number of LB transferred layers of **1**. Quantitative analysis of the molecular orientation requires knowledge of the direction of the transition dipole vector within the molecule. This vector for the ν(C-O) vibration is oriented along the C-O bond.[19] In LB films containing the oxidized form of **1** the average tilt angle of three phenolate groups of the metallosurfactant molecules is close to 60 ° (Figure 5). In the first negative-going potential scan phenolate groups in LB films undergo large changes of their orientation: At E < -0.2 V the tilt of phenolate C-O bonds decreases indicating that Fe^{III} reduction is accompanied by a rotation of the molecule by *ca.* 20 °. In addition, in the LB monolayer the potential- driven desorption and resorption processes lead to further reorientations of the phenolate groups. In the reduced form of **1** the phenolate groups tend to adopt an upwards with respect to the Au surface orientation. Reduction of a small fraction of **1** located close to the Au surface precludes major changes in the orientation of **1** in the 5LB film (**Figure 5b**). During the irreversible reduction reaction the average tilt of the three phenolate groups decreases by *ca.* 50 °. In the reduced form of **1** they tend to be oriented almost normal to the Au surface. No further potential dependent changes are observed. These results support the idea that the reduction of Fe^{III} to Fe^{II} in **1** is accompanied by irreversible changes in the orientation of the C-O groups, which might be reinforced by geometric changes in the molecule structure after reduction of the metal ion and consequent detachment of one phenolate.

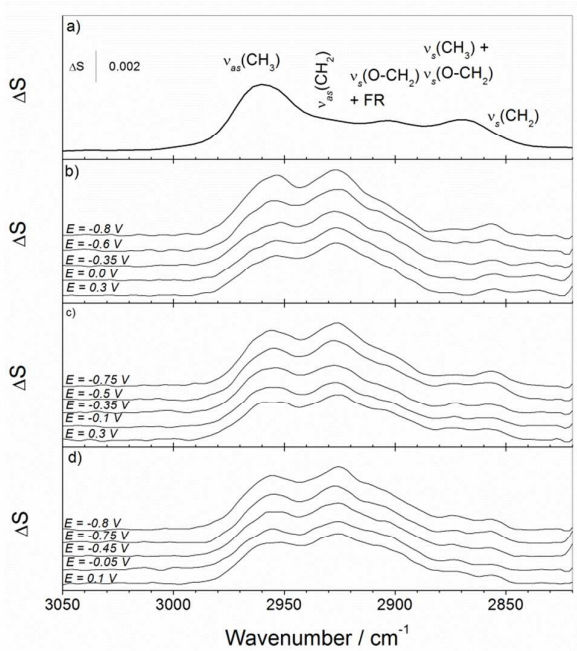

Figure 6a-d. PM IRRA spectra in 3050 – 2700 cm^{-1} spectral region of (a) randomly distributed molecules of **1** in a monolayer thick film and **1** molecules in a LB monolayer on Au surface in (b) first negative-going, (c) subsequent positive and (d) negative-going potential scans at indicated potentials.

Such large localized orientation changes affect the entire molecule of **1**, as evidenced by PM IRRA spectra of the CH stretching modes shown in **Figures 6** and **7** for the monolayer and 5LB samples, respectively. The analysis of this spectral region provides information on the orientation of two hydrophilic alkoxy chains of **1** in LB films. One molecule of **1** contains four benzene rings sharing 20 methyl groups, 4 methylene groups, and 8 CH groups contributing to the IR spectrum CH stretching modes. The broad and intense absorption at 2964 cm^{-1} is due to the $\nu_{as}(CH_3)$ mode. Because **1** is largely comprised of methyl groups, this mode is the strongest in the spectrum of randomly distributed molecules (**Figures 6a** and **7**).

The mode at 2870 cm^{-1} has a complex composition ascribed to the $\nu_s(CH_3)$ in the *tert*-butyl residues, the $\nu_{as}(OCH_2)$ groups and a combination tone of the $\delta(CH_2)$ mode[25] from four methylene groups are associated to the hydrophilic alkoxy chains. The presence of the O atom in this chain influences the frequencies of the methylene stretching modes.[25] The $\nu_{as}(CH_2)$ mode is centered at 2935 cm^{-1} while the $\nu_s(CH_2)$ mode has two contributions at 2900 cm^{-1} and 2865 cm^{-1}. The mode at 2900 cm^{-1} is complex and contains a contribution from the $\nu_s(CH_2)$ mode, as well as from the Fermi resonance between $\nu_s(CH_2)$ and the overtones of the methylene bending mode.[26] The PM IRRA spectra of the monolayer and 5LB films show large changes compared to the spectrum of randomly distributed molecules.

The maximum of the $\nu_{as}(CCH_3)$ absorption mode is centered at 2956 cm^{-1}. However, its relative intensity in *in situ* PM IRRA spectra decreases. By contrast, a broad absorption mode with

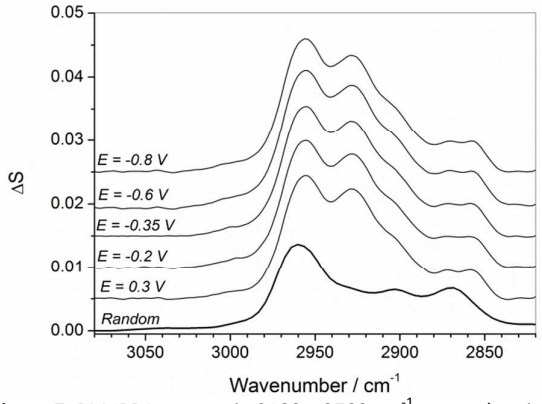

Figure 7. PM IRRA spectra in 3100 – 2700 cm^{-1} spectral region of 5-LB **1** film on the Au electrode surface in the first negative-going potential scan at indicated potentials. A thick line corresponds to a PM-IRRA spectrum calculated for randomly distributed **1** molecules in a 5-LB thick film.

the maximum at 2926 cm^{-1} is significantly enhanced in LB films. Independent of the applied potential, the intense mode at 2926 cm^{-1} (fwhm = 26.3 ± 1.2 cm^{-1}) arises from the $\nu_{as}(CH_2)$ mode. Both the position and the fwhm values indicate that the short hydrocarbon chains in **1** exist in a liquid state.[26, 27] The low frequency side contribution to this broad absorption mode arises from the $\nu_{as}(OCH_2)$ and a Fermi resonance. In the LB films two absorption modes at 2872 and 2856 cm^{-1} are respectively attributed to $\nu_s(CH_3)$ mode and $\nu_s(CH_2)$ modes. As

a consequence of their uniform orientation,[28, 29] the molecules of **1** in LB films demonstrate significantly enhanced intensities in the methylene stretching modes compared to the PM IRRA spectrum of randomly distributed molecules. Qualitative analysis of the chain orientation requires deconvolution of the overlapped IR absorption modes, as shown in **Figure S4** for a monolayer at –0.3 V (adsorbed state) and –0.8 V (desorbed state).

The integral intensities of the $\nu_{as}(CH_2)$ and $\nu_s(CH_2)$ modes in the LB films **1** were used to determine the angle θ between the transition dipole vector of respective modes and the direction of the electric field vector (surface normal) **(Figure 8)**. The transition dipole vectors of the $\nu_{as}(CH_2)$ and $\nu_s(CH_2)$ modes lie in the plane of the methylene group and are perpendicular to each other.[30] The transition dipole vector of the $\nu_s(CH_2)$ mode lies along the bisector of the methylene group while of the $\nu_{as}(CH_2)$ lines along the line joining two H atoms of the methylene group as shown in **Figure 9**a. In the monolayer, $\theta_{\nu as(CH2)}$ and $\theta_{\nu s(CH2)}$ angles depend on the potential applied to the Au electrode. In the first negative-going potential scan a distinct behavior is observed. In other words, at E > -0.2 V the transition dipole vector of the $\nu_{as}(CH_2)$ mode makes an angle $\theta_{\nu as(CH2)}$ of 38° ± 2 ° and the $\theta_{\nu s(CH2)}$ angle of the $\nu_s(CH_2)$ mode varies from 60 ° to 50 °. A further negative potential shift and reduction of Fe^{III} to Fe^{II} on **1** leads to a decrease of the $\theta_{\nu as(CH2)}$ and $\theta_{\nu s(CH2)}$ angles to ca. 15 °. In the subsequent positive-going potential scan, at E > -0.1 V, both angles increase to 40 ° (Fig. 8 a,b).

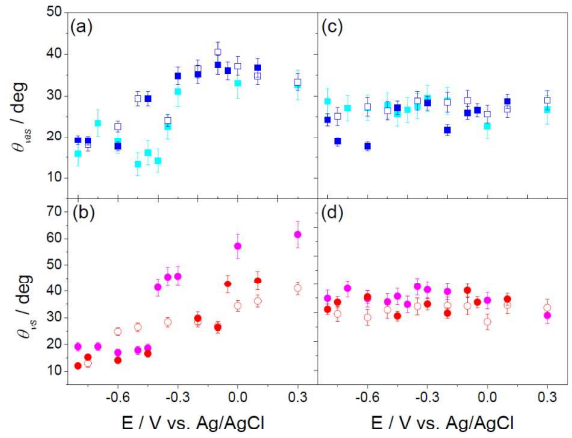

Figure 8a-b. Plots of θ *vs. E* applied to the Au electrode: (a) $\theta_{\nu as}$ (cyan, blue) and (b) $\theta_{\nu s}$ (magenta, red) in LB monolayer of **1** (c) $\theta_{\nu as}$ and (d) $\theta_{\nu s}$ in 5-LB film of **1**. Filled cyan and magenta points: first negative; open blue and red points: subsequent positive and filled blue and red points: subsequent negative

The transition dipole vector of the $\nu_{as}(COC)$ at the ester group joining the metal center with the chains region is oriented along the line between two C atoms determining the tilt of the alkoxy chains (**Figure 9 a**). Thus, it makes a normal angle to the direction of the transition dipole vector of the $\nu_s(CH_2)$ mode. **Figure 9 b** shows the $\theta_{\nu as(COC)}$, $\theta_{\nu s(CH2)}$ angles and their sum in the monolayer of **1** as a function of potential applied to the Au electrode. In the negative-going potential scan, at E > -0.2 V, the $\theta_{\nu as(COC)}$ angle is very small, while the $\theta_{\nu s(CH2)}$ angle is large and close to 60 °. During the reduction reaction of **1** in the LB monolayer, the $\theta_{\nu as(COC)}$ angle increases to 70 ± 7 ° and the $\theta_{\nu s(CH2)}$ angle decreases to *ca.* 20 °. The sum of these two angles adds to 90 ° (**Figure 9**) as expected from the analysis of the orientation of the transition dipole vectors of these two modes.

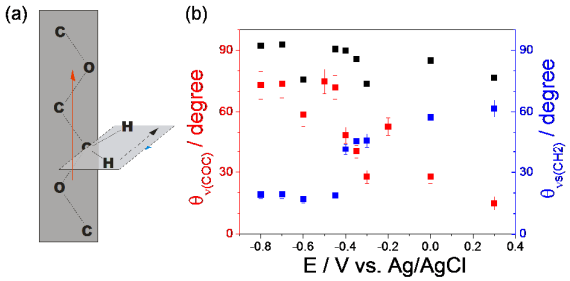

Figure 9a-b. (a) Structure of the alkoxy chain in **1** with marked directions of the transition dipole vectors of the $\nu_{as}(COC)$ (red), $\nu_s(CH_2)$ blue and $\nu_{as}(CH_2)$; (b) Plots of the angle θ vs. E applied to the Au electrode in the first cathodic scan: $\theta_{\nu s(CH2)}$ (blue) and $\theta_{\nu as(COC)}$ (red) of **1** in the monolayer. Black points represent a sum of $\theta_{\nu s(CH2)}$ and $\theta_{\nu as(COC)}$ angles.

The results described above indicate that in the freshly prepared LB monolayer, the alkoxy chains have a small *ca.* 20 ° tilt with respect to the surface normal. Reduction of the metal center is connected with an almost vertical reorientation of the short chains. Their tilt towards the Au surface increases to *ca.* 70°. In the case of the 5-layer LB film, the intensities of the methylene stretching modes are enhanced with minimal dependence on the applied potential (**Figure 8**). The intensity of the $\nu_{as}(COC)$ mode at 1240 cm^{-1} in the multilayer LB film is attenuated (**Figure 4**). The average tilt of the alkoxy chains in **1** is close to 64 ° ± 8°. This orientation is not affected by the Fe^{III} reduction and is similar to the orientation of the alkoxy chains in the post-reduction monolayer. Similarly, *in situ* PM IRRA spectra of the ring stretching modes region of the hydrophobic aromatic groups show negligible spectral changes (**Figure S5**). These modes display differences between the solution spectra of randomly distributed molecules and their LB films (**Figures S5, S6**). For example the ring stretching modes at 1585 and 1555 cm^{-1} are enhanced in LB films whereas the mode at 1512 cm^{-1} is attenuated. The relative intensities of the ring stretching modes also differ between monolayer and 5-LB multilayer films. These differences indicate that **1** shows distinct orientation in monolayer and in multilayer films, where intermolecular interactions along with structural rearrangement during reduction determine the orientation of the molecule in the adsorbed film.

Conclusions

The five-coordinate amphiphilic complex $[Fe^{III}(L^{N2O3})]$, **1**, is capable of diode-like current rectification when deposited as

an LB monolayer between gold electrodes. In this *in situ* spectroelectrochemical study we have investigated by means of PM IRRAS the changes caused by the redox reduction of the Fe^{III}/Fe^{II} pair in **1** in monolayer and 5-layer LB films on gold surfaces aiming to gain insight on the reasons that lead to a gradual decrease in activity after multiple redox cycles.

We observed that electron transfer associated with formation of an Fe^{II} center triggers large reorientation of the adsorbed molecules. At potentials lower than -0.75 V desorption of the film takes place. This was originally thought to be the reason for the observed lack of activity, and may indeed have some long-term consequences. However, the desorpted film is resorpted to the surface of the Au electrode upon reversing the direction of the potential scan. Therefore this process is not considered the main culprit for deactivation.

More concerning was an observed change in orientation of the ligand donors in the vicinity of the metal center, as well as to the hydrophilic alkoxy chains. These sub-molecular regions are strongly dependent on the applied potentials. **Figure 10** illustrates schematically the changes in orientation for **1** in a monolayer during the first negative-going potential scan (reduction). Based on the published structure[1] of **1** and on the orientation of the alkoxy chains discussed above, a scheme is provided on the molecular orientation during the first negative-going potential scan.

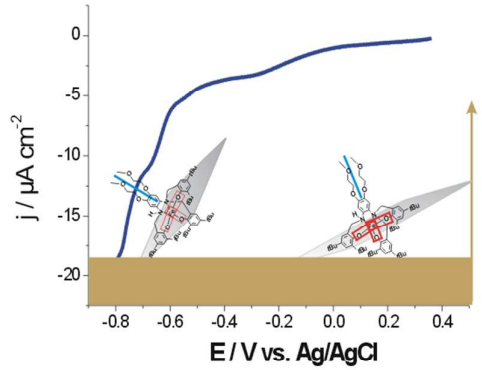

Figure 10. Current density *vs.* potential CV curve of the monolayer of 1 on Au in the negative-going potential scan with a scheme representing the orientation of **1** on the Au surface as a function of potential.

The tilt of the short alkoxy chain in the oxidized form of **1** in the LB monolayer is close to 20 ° *vs.* the surface normal, indicating that they adopt a preferential perpendicular to the Au surface orientation. The phenolate groups preferentially orient parallel to the surface of the electrode. Upon Fe^{III}/Fe^{II} reduction a large reorientation of **1** follows, the alkoxy chains make an angle of ca. 70 ° *vs*. the surface normal (**Figure 10**). This change is caused by the cleavage of at least one of the three Fe-$O_{phenolate}$ bonds. As a consequence the C-O bonds at the phenolate groups adopt a more vertical orietnation towards the Au surface. Even expecting that some of these bonds may be reformed upon reoxidation of the iron center in **1**, we consider this process inseparable with structural alternations and the ultimate cause of deactivation.

The results described in this paper clearly suggest that the electron transfer processes during current rectification may be responsible for dramatic changes in the structure, packing, and orientation of molecules adsorbed on an electrode surface. Although there are many differences between the diode assemblies [1, 2, 6, 7] described for **1** and the experimental conditions of this work, this knowledge is fundamental to identify issues and propose improvements to the design of future metallosurfactants.

Experimental

LB preparation of monolayers and multilayers. $[Fe^{III}(L^{N2O3})]$, **1**, was synthesized according to a published procedure.[2] Monolayers and mutilayers of **1** were prepared on a polycrystalline Au electrode surface using a vertical Langmuir-Blodgett transfer trough. The LB monolayer transfer was done at the air|water interface at a surface pressure of 33 mN m^{-1} and slide withdrawal of 30 mm m^{-1}. The average transfer ratio was equal to 1.18 ± 0.20 for ten independent experiments. The 5-LB layers were transferred at 33 mN m^{-1} with successive withdrawing/immersing cycles and speed transfers between 22 to 30 mm min^{-1}. After immersion the sample was held for 10 minutes in air to dry and stabilize a freshly transferred monolayer. The best transfer ratios were obtained when the speed of the substrate withdrawing was set to 30 and immersing 25 mm min^{-1}. The upwards transfer ratio was equal to 1.08 ± 0.24 and downwards 0.86 ± 0.09. LB films were left for 48 h for drying before their use in electrochemical and PM IRRAS experiments.

Electrochemistry. Electrochemical measurements were performed in an all-glass three-electrode cell with either a polycrystalline Au disc electrode or an evaporated gold film on glass as the working electrode. A gold wire served as the counter electrode and a silver/silver chloride electrode (Ag/AgCl with saturated KCl) as the reference electrode. All potentials are referred against the Ag/AgCl electrode. The reference electrode was separated from the electrolyte solution via a salt bridge. The electrolyte was 0.1 M NaF (Merck, Darmstad, Germany). Prior to the experiment, the cell was purged with argon for 30 minutes. The cleanness of the electrochemical cell was tested by recording cyclic voltammograms in the electrolyte solution. A CHI660A potentiostat (CH Instruments, Austin, USA) with the corresponding software was used to perform the electrochemical measurements. Cyclic voltammograms were recorded between 0.45 and -0.80 V *vs.* Ag/AgCl at different scan rates.

Polarization modulation infrared reflection absorption spectroscopy (PM IRRA). PM IRRA spectra were recorded using a Vertex 70 spectrometer with a polarization modulation set (PMA 50, Bruker, Ettlingen, Germany). All spectra were recorded in a spectroelectrochemical cell at various potentials applied to a polycrystalline gold electrode (disk, diameter 15 mm) which served also as a mirror for the IR light. CaF_2 and

BaF_2 equilateral prisms were used as an optical window for the IR radiation. Before assembly of the spectroelectrochemical cell, the prism was washed with water, ethanol and cleaned for 10 minutes in an ozone chamber (Bioforce Nanosciences, Ames, USA). Monolayer and 5-multilayer films of the **1** complex were transferred onto a gold disc electrode. The spectroelectrochemical cell has built-in platinum counter electrode. The reference electrode was Ag/AgCl in 3M KCl in D_2O (H_2O). The cell was filled with 0.05 M NaF electrolyte in either D_2O or H_2O and purged with argon for 1h to remove oxygen. At each potential applied to the Au electrode 2500 spectra with a resolution of 4 cm^{-1} were recorded. In each experiment three cathodic (negative-going) and anodic (positive-going) potential scans were recorded. Each potential scan was analyzed separately. In the cathodic potential scan the following potentials were applied to the Au electrode 0.3, 0.2, 0.0, -0.2, -0.3, -0.4, -0.5, -0.6, -0.8 V *vs.* Ag/AgCl while in the anodic potential scan -0.6, -0.5, -0.4, -0.3, -0.2, 0.0, 0.2 and 0.3 V *vs.* Ag/AgCl. For the analysis of the CH stretching bands, the maximum PEM efficiency was set for the half-wave retardation equal to 2900 cm^{-1}. The thickness of the electrolyte layer between the CaF_2 prism and the Au electrode was d = 1.8 ± 0.2 μm. The angle of incidence of the IR light φ = 52°. At the half-wave retardation set to 1600 cm^{-1} the CC stretching modes at the aromatic rings were analyzed; φ = 60 ° and d ≈ 3.2 ± 0.4 μm. In these experiments D_2O was used as a solvent. For the analysis of the C-O stretching modes, the PEM efficiency was set for the half-wave retardation equal to 1200 cm^{-1}. The thickness of the electrolyte layer between the BaF_2 prism and the Au electrode was d = 4.0 ± 0.4 μm. The angle of incidence of the IR light φ = 57°. The background correction of PM IRRA spectra was done using the OPUS v5.5 software (Bruker, Ettlingen, Germany). Spectra shown in this paper show absorbance from the organic molecules present on the metal surface, as calculated after the background subtraction and normalization (ΔS) as a function of wavenumbers. [31] Each set of experiments was performed three times. Spectra presented in this paper correspond to average figure obtained from three independent measurements.

Fourier-transform Infrared Spectroscopy (FT IRS). *FT IRS* spectra in the transmission mode of complex **1** dissolved in CCl_4 (Aldrich, Steinheim, Germany) were measured using a flow cell (Aldrich). The solution (background) spectrum was measured in a 25 μm thick thin flow cell in which a Teflon spacer was placed between two ZnSe optical windows. After the measurement of the background spectrum a sample spectrum of the analyte dissolved in CCl_4 was measured. Transmission spectra were used to determine the optical constants as described in detail in the literature.[15, 31]

Conflicts of interest

There are no conflicts to declare.

Acknowledgements

The authors acknowledge support from the DAAD (grant 57215882 to IB, which facilitated academic exchange with Poland and hosting of JJD at the University of Oldenburg), the National Science Foundation (grants NSF-CHE1012413 and NSF-CHE-1500201 to CNV), including financial support to LW.

References:

1. L. D. Wickramasinghe, M. M. Perera, L. Li, G. Mao, Z. Zhou and C. N. Verani, *Angew. Chem. Int. Ed.*, 2013, **52**, 13346-13350.
2. L. D. Wickramasinhe, S. Mazumder, S. Gonawala, M. Madusanka Perera, H. Baydoun, B. Thapa, L. Li, L. Xis, G. Mao, Z. Zhou, H. B. Schlegel and C. N. Verani, *Angew. Chem. Int. Ed.*, 2014, **53**, 14462-14467.
3. L. D. Wickramasinghe, S. Mazumder, K. K. Kpogo, R. J. Staples, H. B. Schlegel and C. N. Verani, *Chem. Eur. J.*, 2016, **22**, 10786-10790.
4. M. S. Johnson, L. D. Wickramasinghe, C. N. Verani and R. M. Metzger, *J. Phys. Chem. C*, 2016, **120**, 10578-10583.
5. S. Dongmo, G. Wittstock, J. Christoffers and I. Brand, *Electrochim. Acta*, 2017, **255**, 198-208.
6. M. M. Allard, J. A. Sonk, M. J. Heeg, B. R. McGarvey, H. B. Schlegel and C. N. Verani, *Angew. Chem. Int. Ed.*, 2012, **51**, 3178-3182.
7. M. Lanznaster, H. P. Hratchian, M. J. Heeg, B. R. McGarvey, H. B. Schlegel and C. N. Verani, *Inorg. Chem.*, 2006, **45**, 955-957.
8. S. Gonawala, H. Baydoun, L. Wickramasinghe and C. N. Verani, *Chem.Comm.*, 2016, **52**.
9. B. Adam, E. Bill, E. Bothe, B. Goerdt, G. Haselhorst, K. Hildenbrand, A. Sokolowski, S. Steenken, T. Weyhermiiller and K. Wieghardt, *Chem. Eur. J.*, 1997, **3**, 308-319.
10. A. Sokolowski, B. Adam, T. Weyhermüller, A. Kikuchi, K. Hildenbrand, R. Schnepf, P. Hildebrandt, E. Bill and K. Wieghardt, *Inorg. Chem.*, 1997, **36**, 3702-3710.
11. S. Gentil, D. Serre, C. Philouze, M. Holzinger, F. Thomas and A. Le Goff, *Angew. Chem. Int. Ed.*, 2016, **55**, 2517-2520.
12. T. Kurahashi, Y. Kobayashi, S. T. Nagatomo, T., T. Kitagawa and H. Fujii, *Inorg. Chem.*, 2005, **44**, 8156-8166.
13. R. Chetty, P. A. Christensen and B. T. Golding, *Chem.Comm.*, 2003, **8**, 984-985.
14. I. Zawisza, I. Burgess, G. Szymanski, J. Lipkowski, J. Majewski and S. Satija, *Electrochim. Acta*, 2004, **49**, 3651-3664.
15. D. L. Allara, A. Baca and C. A. Pryde, *Macromolecules*, 1978, **11**, 1215-1220.
16. M. D. Snodin, L. Ould-Moussa, U. Wallmann, S. Lecomte, V. Bachler, E. Bill, H. Hummel, T. Weyhermüller, P. Hildebrandt and K. Wieghardt, *Chem. Eur. J.*, 1999, **5**, 2554-2565.
17. A. Sokolowski, J. Mueller, T. Weyhermüller, R. Schnepf, P. Hildebrandt, K. Hildenbrand, E. Bothe and K. Wieghardt, *J. Am. Chem. Soc.*, 1997, **119**, 8889-8900.
18. C. Berthomieu and A. Boussac, *Biospectrosocpy*, 1995, **1**, 187-206.
19. V. S. Griffiths and G. A. W. Derwish, *J. Mol. Spectrosc.*, 1962, **9**, 83-94.

20. R. P. Dain, G. Gersham, G. S. Groenewold, J. F. Steill, J. Oomens and M. J. van Stipdonk, *Rapid Commun. Mass Spectrom.*, 2011, **25**, 1837-1846.
21. A. Mukherjee, M. L. McGlashen and T. G. Spiro, *J. Phys. Chem.*, 1995, **99**, 4912-4917.
22. D. Sajan, K. P. Laladhas, I. Hubert Joe and V. S. Jayakumar, *J. Raman Spectrosc.*, 2005, **36**, 1001-1011.
23. M. Moskovits, *J. Chem. Phys.*, 1982, **77**, 4408-4416.
24. R. J. Lippert, B. D. Lamp and M. D. Porter, in *Modern techniques in Applied Molecular Spectroscopy*, ed. F. M. Mirabella, John Wiley and Sons, Inc., New York, Editon edn., 1998, pp. 83-126.
25. T. Miyazawa, K. Fukushima and Y. Ideguchi, *J. Chem. Phys.*, 1962, **37**, 2764-2776.
26. R. A. MacPhail, H. L. Strauss, R. G. Snyder and C. A. Elliger, *J. Phys. Chem.*, 1984, **88**, 334-341.
27. R. G. Snyder, H. L. Strauss and C. A. Elliger, *J. Phys. Chem.*, 1982, **86**, 5145-5150.
28. D. L. Allara and R. G. Nuzzo, *Langmuir*, 1985, **1**, 52-66.
29. D. L. Allara and J. D. Swalen, *J. Phys. Chem.*, 1982, **86**, 2700-2704.
30. U. P. Fringeli, *Z. Naturforsch.*, 1977, **32c**, 20-45.
31. V. Zamlynny and J. Lipkowski, in *Adv. Electrochem. Sci. Eng.*, eds. R. C. Alkire, D. M. Kolb, J. Lipkowski and P. N. Ross, Wiley-VCH, Weinheim, Editon edn., 2006, vol. 9, pp. 315-376.

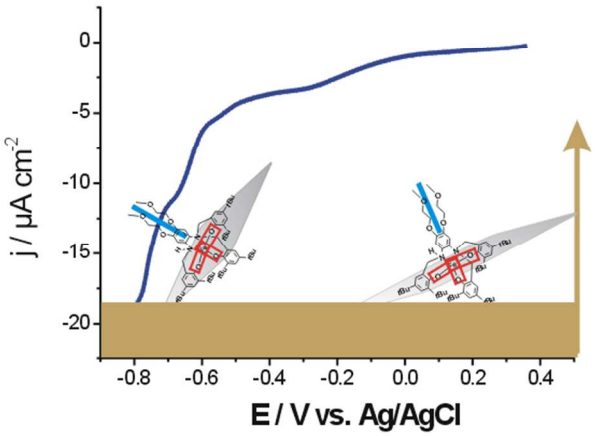

An iron metallosurfactant in Langmuir-Blodfett films undergoes reduction which is accompanied by pronounced structural rearrangements of the adsorbed molecule.